Spatial Characteristics of 3D MIMO Wideband Channel in Indoor Hotspot Scenario at 3.5 GHz

Lei Tian, Jianhua Zhang, Yuxiang Zhang
State Key Lab. of Networking and Switching Tech.,
Beijing Univ. of Posts and Telecom., China.
tianlbupt@bupt.edu.cn, jhzhang@bupt.edu.cn,
zhangyx@bupt.edu.cn

Yi Zheng
China Mobile Communications Corporation, China.
zhengyi@chinamobile.com

***Abstract*—Three dimension (3D) Multiple Input and Multiple Output (MIMO) with massive antenna elements, due to the advantage of using elevation domain than 2D MIMO, is regarded as a promising technique for the fifth generation (5G) mobile communication systems. This makes the channel characteristics of elevation domain as a basic requirement for the 5G channel model. In this paper, we conducted a 3D MIMO channel measurement at 3.5 GHz with 100 MHz bandwidth in indoor hotspot scenario which is one of the important scenario for 5G. Based on the channel measurement data, spatial characteristics of elevation domain are analyzed and discussed, including power angular spectrum, angular spread, and cross-correlation, etc. The extracted channel parameters of elevation domain can be used in the 3D MIMO technology evaluation and simulation for indoor hotspot scenario.**

***Index Terms*—3D MIMO, channel measurement, indoor hotspot, elevation angle**

I. INTRODUCTION

With the rapid and tremendous growing of the volume of mobile traffic, the fifth generation (5G) mobile communication system, also named as IMT-2020 by International Telecommunication Union Radio-communication Sector (ITU-R), aims at higher user data rate, short transmission latency, and low energy consumption, etc. has aroused great attention all over the world [1]. In order to reach these requirements, three dimension (3D) Multiple Input and Multiple Output (MIMO) is considered to be one of the most promising and practical technique. MIMO technique has been introduced into the fourth generation mobile communication system and improved the system spectrum efficiency to a large extent by utilizing the channel spatial degree of freedom. Compared with the traditional MIMO, 3D MIMO, especially with massive antenna elements, can take full use of the spatial channel resources by introducing the elevation domain [2].

One of the fundamental work to evaluate and utilize 3D MIMO technique is to extend the 2D channel to 3D with adding the elevation domain characteristics. A lot of research has been focusing on the 3D MIMO channel to establish a reliable and precise 3D channel model [3-8]. The report of Word Wireless Initiative New Radio + (WINNER+) summarise some measurement results of the elevation angle of arrival (EoA) at mobile station (MS) side and corresponding elevation angle of departure (EoD) at base station (BS) side for various scenarios [3]. most of the studies pay attention to the 3D channel in outdoor scenarios like Urban Macro (UMa) and Urban Micro (UMi), and outdoor-to-indoor (O2I) scenario. [7] analyzes the angular spread and offset in elevation domain based on the measurement in Urban environment, whereas [6] and [8] focus on the elevation characteristics in O2I scenario. In early 2014, the 3rd Generation Partner Project (3GPP) issued a technical report TR 36.873 which is a 3D MIMO channel model contributed by lots of companies [9]. However, the report only contains the 3D channel model for UMa, UMi, and O2I scenario. Thus, there is few study on the 3D channel of indoor hotspot (InH) scenario.

InH scenario referred to the environment with large quantities of users and big mobile traffic load, such as shopping mall, train station, and airport, is one of the most important scenario for IMT-2020. Therefore, considering that the knowledge of 3D channel is indispensable to develop 3D MIMO in InH scenario, we conducted the 3D channel measurement campaign at 3.5 GHz with 100 MHz bandwidth in order to obtained the spatial characteristics of elevation domain in InH scenario. The extracted elevation angle parameters could support the evaluation and simulation of 3D MIMO technique.

The remainder of the paper is organized as follows. The channel measurement system and scenario plan are described in Section II. Then, the data processing procedure is explained in Section III. In Section IV, the channel characteristics of elevation domain of InH scenario are analyzed and discussed in detailed. Finally, the conclusion is drawn in Section V.

II. Channel Measurement Description

A. Measurement System

The measurement campaign was conducted at a center frequency of 3.5 GHz with 100MHz bandwidth by using the Elektrobit Propsound channel sounder [10]. An auto-swicthing unit is equipped both at transimtter (Tx) and receiver (Rx) to control the periotic pseudo random (PN) binary signal transmitting between the Tx and Rx antenna paris in a time division multiplexing mode. One time period in which all the sub-channels are sounded once is regarded as a measurement cycle (snapshot).

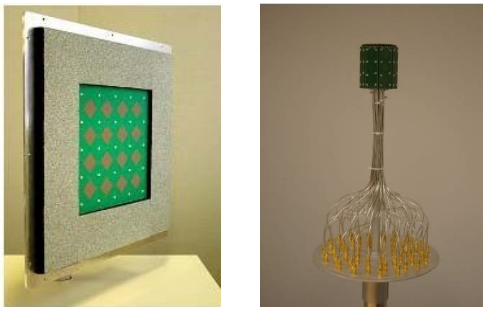

Fig. 1. Antenna arrays used at Tx (UPA) and Rx (ODA).

3D antenna arrays are chosen to capture the 3D channel responses. A uniform planr array (UPA) is applied at Tx, whereas a omni-directional antenna array is utilized at Rx. As illustrated in Fig.1, the UPA consists of totally 16 antenna patches which are placed uniformly in a 4×4 square. Each antenna patch is a dual-polarized antenna connected with two antenna ports. The ODA has 28 antenna patches 24 of which are arranged in 8 adjacent sides with 3 in each side, 4 or which are on the top. The detailed antenna specification and system configuration are listed in Table I.

TABLE I. Antenna specification and system configuration

Configuration Item		**Value**	
Antenna type of Tx / Rx		UPA	ODA
Number of antenna elements		32	56
Polarization		±45°	±45°
Angular range of antenna	Horizontal	−70° ~ 70°	−180° ~ 180°
	Vertical	−70° ~ 70°	−70° ~ 90°
Center frequency		3.5 GHz	
Bandwidth		100 MHz	
Length of PN code		255	
Tx power		33 dBm	

B. Measurement scenario

The InH scenario is selected in the hall of the third teaching building of Beijing University of Posts and Telecommunications. Fig. 2 shows the layout of the InH measurement area. The Tx regarded as base station (BS), marked by the red triangle, is located in the center of the lobby of the first floor with the antenna height of 2.61 m. The Rx antenna with the height of 1.7 m is set up on a trolley. The Rx represented by mobile station (MS) are marked by yellow and gray triangles for line-of-sight (LoS) and non-line-of-sight (NLoS), respectively. A total of 60 Rx locations are selected, and 500 snapshots are collected at each Rx location.

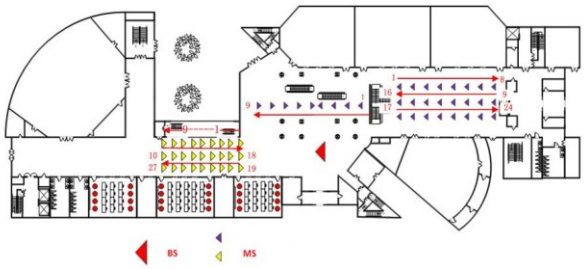

Fig. 2. Measurement plan of InH scenario.

III. Data Processing

After the field channel measurement, channel impuls responses (CIRs) are firstly be calculated from the raw channel data. It is assumed that the number of Tx and Rx antenna elements are M and N, respectively. Then, the number of sub-channel is $M\times N$, which is 32×56 in our measurement.

A. SAGE Algorithm

After we obtain CIRs, the space alternative generalized expectation maximization (SAGE) algorithm is utilized to extract the multi-path channel parameters due to its high precision and low computaion complexity [11][12]. The SAGE algorithm provides a joint estimation parameter set of the l th path, which can be written as

$$\eta_l = \left\{\mathbf{A}_l, \tau_l, \phi_{rx,l}, \theta_{rx,l}, \phi_{tx,l}, \theta_{tx,l}, \nu_l\right\}, \quad l = 1,\cdots \tag{1}$$

The $\mathbf{A}_l$, τ_l, and ν_l denote the complex polarization matrix, propagation delay, and doppler shift of the l th path. Especially, $\phi_{rx,l}$ and $\theta_{rx,l}$ represent the azimuth and elevation angles of arrival at Rx side, whereas $\phi_{tx,l}$ and $\theta_{tx,l}$ are the corresponding angles of departure at Tx side. L is the maximum number of resolvable path to be estimated. It is empirically set to 120, which gauratees that the paths with the strongest power can be extracted from the measurement data.

B. Power Angular Spectrum

As we have obtained the parameter set of each path, the power of each path can be calculated by

$$P_l = \sum_{p_1=1}^{2}\sum_{p_2=1}^{2}\left|\alpha_{l,p_1,p_2}\right|^2, \tag{2}$$

where α_{l,p_1,p_2} is the polarization coefficient in $\mathbf{A}_l$ .Then the power angular spectrum (PAS) is written as

$$f(\varphi)=\sum_{l=1}^{L}\delta(\varphi-\varphi_l)P_l, \tag{3}$$

where φ_l could be $\phi_{rx,l}$, $\theta_{rx,l}$, $\phi_{tx,l}$ or $\theta_{tx,l}$. Then the PAS of AoA, EoA, AoD, or EoD can be obtained correspondingly. In this paper, we mainly focuse on the PAS of elevation angle. Generally, Laplacian distribution is used to fit the elevation angle PAS, whose prorability distribution function is given as

$$f(x)=\frac{1}{\sqrt{2}\sigma}\exp\left(-\frac{\sqrt{2}}{\sigma}|x-\mu|\right), \tag{4}$$

where μ and σ denotes the mean and standard deviation of Laplacian distribution, respectively.

C. Anglular Spread

Root-mean-square angular spread (rms AS) is an important parameter to characterize the dispersion in spatial domain of multi-path components. It is the second central moment of PAS. In order to avoid the angle ambuguity, the circular anglular spread (CAS) is often used and can be calculated by

$$\sigma_{\mathrm{CAS}}=\min_{\Delta}\sigma_{\mathrm{AS}}(\Delta)=\min_{\Delta}\sqrt{\frac{\sum_{l=1}^{L}\left(\varphi_l(\Delta)-\mu(\Delta)\right)^2P_l}{\sum_{l=1}^{L}P_l}}, \tag{5}$$

where $\varphi_l(\Delta)=\varphi_l+\Delta$. represent the shifted angle with certain angular shift of Δ . $\mu(\Delta)$ are defined as

$$\mu(\Delta)=\frac{\sum_{l=1}^{L}\varphi_l(\Delta)P_l}{\sum_{l=1}^{L}P_l}. \tag{6}$$

It should be noted that both $\varphi_l(\Delta)$ in (6) and $\varphi_l(\Delta)-\mu(\Delta)$ in (10) are normlized according to

$$\beta=\begin{cases}2\pi+\beta, & \text{if } \beta<-\pi\\ \beta, & \text{if } |\beta|\le\pi\\ 2\pi-\beta, & \text{if } \beta>\pi\end{cases}. \tag{7}$$

D. Cross-correlation of parameters

As the elevation angle is introduced to the channel model, the cross-correlations of elevation angle with other channel parameters including shadow fading (SF), Ricean K factor, delay spread (DS), and azimuth angular spread of departure and arrival (ASD, ASA) are required. The cross-correlation coefficient of two channel parameters X and Y can be calculated by

$$\rho_{XY}=\frac{\mathrm{E}\left(\left(X-\mathrm{E}(X)\right)\left(Y-\mathrm{E}(Y)\right)\right)}{\sigma_X^2\sigma_Y^2}, \tag{8}$$

where σ_X^2 and σ_Y^2 dontes the variance of X and Y , respectively.

IV. Results and Analysis

A. PAS of Elevation Angle

The PASs of EoD and EoA for LoS and NloS cases are illustrated in Fig. 3. It can be observed that The elevation angle is fitted by the Laplacian distribution well. It shows the same with the elevation angle distribution of UMa and UMi defined in [9].

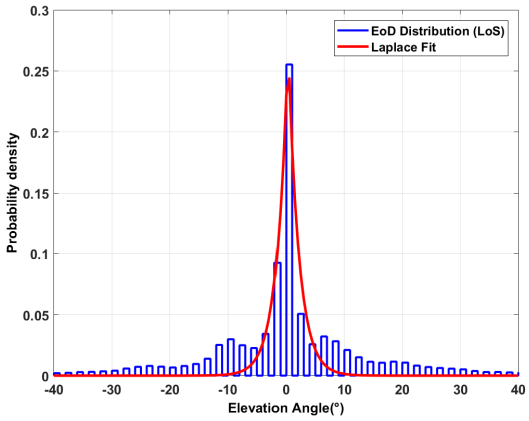

(a) PAS of EoD in LoS InH

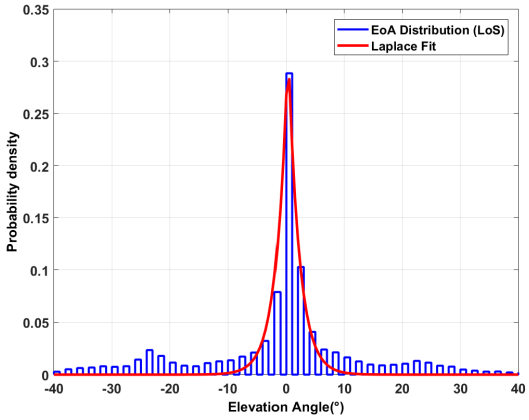

(b) PAS of EoA in LoS InH

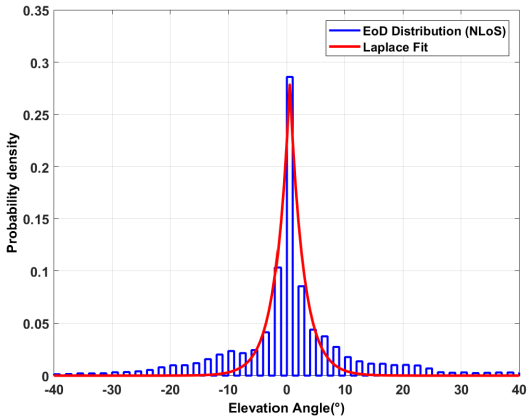

(c) PAS of EoD in NLoS InH

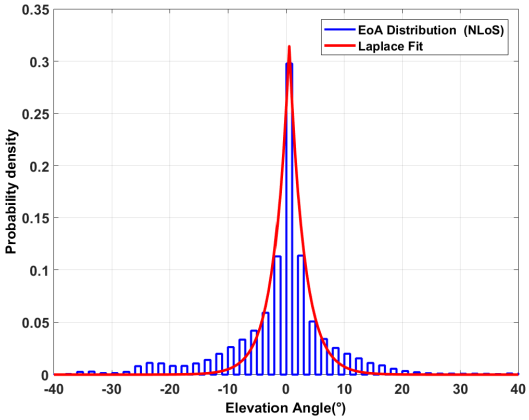

(d) PAS of EoA in NLoS InH

Fig. 3. PAS of elevation angle.

B. Elevation Angular Spread

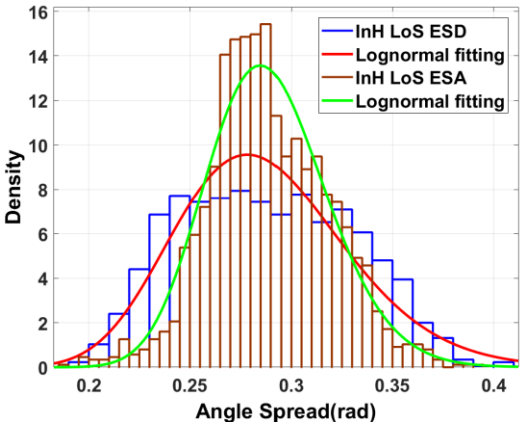

Fig. 4. Lognormal fit for ESD and ESA distribution in LoS InH.

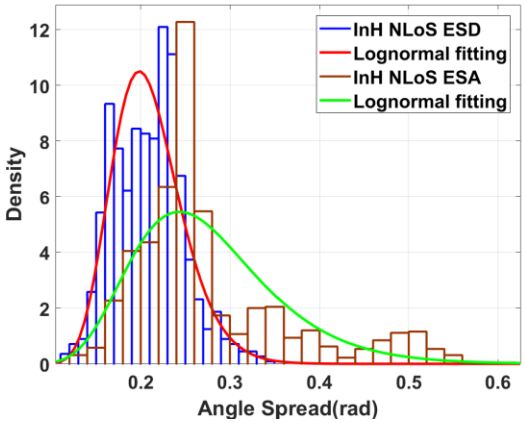

Fig. 5. Lognormal fit for ESD and ESA distribution in NLoS InH.

Fig. 4 and 5 shows the distribution of ESD and ESA in LoS and NLoS cases, respectively. Lognormal distribution is used and found to fit the distribution of ESD and ESA well. The same distribution is also used for DS, ASA, and ASD distribution fitting in [9]. The mean value and standard deviation of the ESD and ESA distribution is given in Table II. The mean ESD in NloS case is larger than that in LoS case. So is the mean ESA. However, the difference of ESD or ESA between LoS and NloS is silight. This reflects the elevation angle can be restricted to some extent by the floor and ceiling in the indoor environment. Comparing the results of indoor office in [3] with the measured results, we can further demonstrate the conclusion that the elevation angular sparead could decrease with the indoor space becoming smaller.

TABLE II. ESD AND ESA STATISTICS IN LOS/NLOS INH SCENARIO

Angular Spread			**Indoor Hotspot**	
			LoS	***NLoS***
Measured InH	ESD $\log_{10}([\text{degree}])$	μ	1.02	1.08
		σ	0.41	0.36
	ESA $\log_{10}([\text{degree}])$	μ	1.22	1.26
		σ	0.23	0.67
WINNER + Indoor Office [3]	ESD $\log_{10}([\text{degree}])$	μ	0.88	1.06
		σ	0.31	0.21
	ESA $\log_{10}([\text{degree}])$	μ	0.94	1.10
		σ	0.26	0.17

C. Cross-correlation of channel parameters

Except for distribution of elevation angle and elevation angular spread, the cross-correlation is also needed when generating the 3D channel model. Table III gives out the cross-correlation of elevation angle with other important channel parameters both in LoS and NLoS case. It can be seen from Table I that the ESD is generally higher correlated with ASD than with other parameters both in LoS and NLoS cases. The similar relation can also be found between ESA and ASA. This

interprets that the azimuth angle and elevation angle at either terminal (BS or MS side) are more likely to change with each other correspondingly.

TABLE III. CROSS-CORRELATION OF ELEVATION ANGULAR SPREAD WITH OTHER PARAMETERS IN LOS AND NLOS OF INH SCENARIO

Cross-correlation	Indoor Hotspot	
	LoS	***NLoS***
ESD vs SF	0.2	0
ESA vs SF	0.3	0
ESD vs K	0	N/A
ESA vs K	0.1	N/A
ESD vs DS	0.1	-0.27
ESA vs DS	0.2	-0.06
ESD vs ASD	0.5	0.35
ESA vs ASD	0	0.23
ESD vs ASA	0	-0.08
ESA vs ASA	0.5	0.43
ESD vs ESA	0	0.42

V. CONCLUSION

As 3D MIMO technique is important to enhance the throughput in InH scenario, it is definitely necessary to extend the 2D channel to 3D with adding the elevation angle parameters. Thus, we performed an 3D MIMO wideband channel measurement at 3.5 GHz with 100 MHz bandwidth in InH scenario including both LoS and NLoS cases. Further, the PAS, angular spread, and cross-correlation of elevation angle are analyzed. The distributions of EoD and EoA obey Laplace distribution, which are similar to those of UMa and UMi scenarios. The ESD and ESA can be modeled as lognormal distribution. Also, the cross-correlation of ESD and ESA with other parameters are provided. The elevation angle parameters in this paper can be used to extend the 2D InH channel model to 3D channel so as to support the 3D MIMO technique evaluation and simulation.

ACKNOWLEDGMENT

The research is supported by National Key Technology Research and Development Program of the Ministry of Science and Technology of China (NO. 2012BAF14B01), National Science and Technology Major Project of the Ministry of Science and Technology (NO. 2015ZX03002008), Ministry of Education-CMCC Science and Research Fund (MCM20160105). The research is also supported by the Exploratory Project of State Key Lab of Networking and Switching Technology (NST20170205).

REFERENCES

[1] ITU-R M.2038, “IMT-Vision – Framework and overall objectives of the future development of IMT for 2020 and beyond,” Sept., 2015.

[2] M. Shafi, A. F. Molisch, P. J. Smith, T. Haustein, P. Zhu, P. De Silva, F. Tufvesson, A. Benjebbour, and G. Wunder, “5G: A tutorial overview of standards, trials, challenges, deployment and practice,” IEEE Journal on Selected Areas in Communications, 2017.

[3] “Wireless world initiative new radio + (WINNER+) D5.3 final channel models,” https://www.ist-winner.org., 2010

[4] J. Zhang; Y. Zhang; Y. Yu; R. Xu; Q. Zheng; P. Zhang, “3D MIMO: How Much Does It Meet Our Expectations Observed from Massive Channel Measurements?,” in IEEE Journal on Selected Areas in Communications, 2017.

[5] J. Zhang, C. Pan, F. Pei, G. Liu, and X. Cheng, “Three-dimensional fading channel models: A survey of elevation angle research,” IEEE Communications Magazine, vol. 52, no. 6, pp. 218-226, 2014.

[6] V. Kristem, S. Sangodoyin, C. Bas, M. Kaske, J. Lee, C. Schneider, G. Sommerkorn, J. Zhang, R. Thoma, and A. Molisch, “3D MIMO outdoor to indoor macro/micro-cellular channel measurements and modeling,” in 2015 IEEE Global Communications Conference (GLOBECOM), pp.1-6, 2015.

[7] F. Pei, J. Zhang, C. Pan, “Elevation angle characteristics of Urban wireless propagation environment at 3.5 GHz,” in 2013 IEEE Vehicular Technology Conference (VTC-fall’13), Sept. 2013.

[8] Y. Yu, J. Zhang, M. Shafi, P. A. Dmochowski, M. Zhang and J. Mirza, "Measurements of 3D channel impulse response for outdoor-to-indoor scenario: Capacity predictions for different antenna arrays," 2015 IEEE 26th Annual International Symposium on Personal, Indoor, and Mobile Radio Communications (PIMRC), Hong Kong, 2015, pp. 408-413.

[9] 3GPP TR 36.873, “Study on 3D channel model for LTE (Release 12),”, 2014.

[10] “Propsound multidimensional channel sounder.” [Online]. Available: http://www.propsim.com.

[11] B. H. Fleury, P. Jourdan and A. Stucki, “High-resolution channel parameter estimation for MIMO applications using the SAGE algorithm,” 2002 International Zurich Seminar on Broadband Communications Access - Transmission - Networking (Cat. No.02TH8599), Zurich, 2002, pp. 30-1-30-9.

[12] X. Yin, B. H. Fleury, P. Jourdan and A. Stucki, “Polarization estimation of individual propagation paths using the SAGE algorithm,” in 14th IEEE Proceedings on Personal, Indoor and Mobile Radio Communications (PIMRC 2003), 2003, pp. 1795-1799.